Biointerphases (2012) 7:43
DOI 10.1007/s13758-012-0043-9

ARTICLE

Reversible Changes in Cell Morphology due to Cytoskeletal Rearrangements Measured in Real-Time by QCM-D

Nina Tymchenko · Erik Nilebäck · Marina V. Voinova · Julie Gold · Bengt Kasemo · Sofia Svedhem

Received: 24 April 2012 / Accepted: 21 June 2012 / Published online: 12 July 2012

Abstract The mechanical properties and responses of cells to external stimuli (including drugs) are closely connected to important phenomena such as cell spreading, motility, activity, and potentially even differentiation. Here, reversible changes in the viscoelastic properties of surface-attached fibroblasts were induced by the cytoskeleton-perturbing agent cytochalasin D, and studied in real-time by the quartz crystal microbalance with dissipation (QCM-D) technique. QCM-D is a surface sensitive technique that measures changes in (dynamically coupled) mass and viscoelastic properties close to the sensor surface, within a distance into the cell that is usually only a fraction of its size. In this work, QCM-D was combined with light microscopy to study in situ cell attachment and spreading. Overtone-dependent changes of the QCM-D responses (frequency and dissipation shifts) were first recorded, as fibroblast cells attached to protein-coated sensors in a window equipped flow module. Then, as the cell layer had stabilised, morphological changes were induced in the cells by injecting cytochalasin D. This caused changes in the QCM-D signals that were reversible in the sense that they disappeared upon removal of cytochalasin D. These results are compared to other cell QCM-D studies. Our results stress the combination of QCM-D and light microscopy to help interpret QCM-D results obtained in cell assays and thus suggests a direction to develop the QCM-D technique as an even more useful tool for real-time cell studies.

N. Tymchenko and E. Nilebäck made equal contributions to this study.

Electronic supplementary material The online version of this article (doi:10.1007/s13758-012-0043-9) contains supplementary material, which is available to authorized users.

N. Tymchenko · E. Nilebäck · J. Gold · B. Kasemo · S. Svedhem (✉)
Department of Applied Physics, Chalmers University of Technology, 412 96 Göteborg, Sweden
e-mail: sofia.svedhem@chalmers.se

E. Nilebäck
Q-Sense, Hängpilsgatan 7, 426 77 Västra Frölunda, Sweden

M. V. Voinova
Department of Microtechnology and Nanoscience, Chalmers University of Technology, 412 96 Göteborg, Sweden

1 Introduction

The mechanical properties and responses of cells, often termed mechanosensing or mechanotransduction, are tightly linked to cell fate processes [1]. The cells have many ways to measure and manipulate mechanical forces, and they respond to, e.g., the rigidity of the underlying substrate [2], topographical cues and constraints [3], and externally applied forces to cells [4–6]. An emerging analytical technique to study properties and responses of cells is the quartz crystal microbalance with dissipation monitoring (QCM-D) technique which is sensitive to nanomechanical properties at an interface [7]. QCM-D is an acoustic surface sensitive method monitoring (1) changes in mass near the sensor surface as a shift in the resonance frequency (Δf) of the sensor crystal and (2) changes in viscoelastic (e.g., stiffness) properties of the adlayer via changes in the damping, or equivalently, the energy dissipation (ΔD) of the shear oscillation of the sensor. Based on such results, the viscoelastic properties of layers formed onto the sensor can be modeled [8–14]. In the cell study area, QCM-D has mostly been used for the development of organic surface modifications, often called functionalised surfaces, intended for biological applications like

biomaterials for medical implants, i.e., before cells were added to these surfaces. These studies have typically been focused on the adsorption of protein layers [15–18], surface functionalisation by coupling of peptides [19–21], the formation of supported lipid bilayers [19, 20, 22, 23], or the properties of layer-by-layer structures based on biopolymers [24]. However, QCM has also been applied as a primary tool for studying of the cells themselves and their surface interactions (recently reviewed in [25]). These studies have been performed both by conventional QCM, without monitoring the dissipation, and by QCM-D. In the early QCM studies, changes in resonance frequency were correlated with osteoblast surface coverage, up to a cell monolayer thickness [26]. QCM was also used to detect effects of different agents on cell viability, sensing the detachment of cells from the sensor [27]. In both these cases, the QCM signals were correlated, and in a way validated, with microscopy performed in separate experiments. The development of QCM-D led to studies of cells where *D*–*f* plots (frequency plotted vs. dissipation), were introduced and used to derive information about cell attachment to substrates [28]. These plots could provide unique signatures or fingerprints, independent of the spatial distribution of cells over the sensor surface for different surfaces [29], and had distinct regimes, which were indicative of the properties on the surface [30]. Thus, it was concluded that several different events could be detected in QCM-D, from initial cell binding through secretion of proteins, cell spreading, changes in adhesion, and changes in the cytoskeleton [30]. Newer studies with QCM-D have included cell adhesion to different metals [31], charged surfaces [32], peptide-functionalised polymer films [33], but also extra-cellular matrix remodelling during cell adhesion [34]. Notable and recent real-time QCM-D measurements on cells include in situ treatments to induce changes in the cell. For example, in one study cell rounding, shrinkage and lysis were induced and studied in conjunction with fluorescence images [35]. In another study cytoskeletal remodelling induced by epidermal growth factor receptor signaling was monitored [36], and recently extended to include atomic force microscopy measurements of changes in individual cells (e.g., providing information about the local cytoskeleton properties) [37].

It is notable when comparing the results reported in the growing number of QCM and QCM-D (or similar) studies involving cells, that there is still no clear picture of what kind of signals in f and D that should be expected from cells on surfaces, neither with respect to the magnitude nor the sign of those f and/or D shifts. Cells ($Ø \approx 10$ μm) occupy a niche where the QCM-D results are, e.g., strongly influenced by the thickness of the sample, which we referred to as a missing mass effect [38, 39]. This is not surprising; a cell layer constitutes a very complex entity as seen from the QCM-D theory and modelling perspective. It is heterogeneous both perpendicular and parallel to the sensor surface and the sensing depth, in most cases much less than the cell thickness, may vary depending on cell properties. Thus, unlike thin (nm) rigid films where a negative frequency shift is proportional to an increase in the adsorbed mass (acoustically coupled water included), the signals from cells require more advanced modelling. It should be noted that even in the absence of such modelling, QCM-D has been demonstrated (see above) to be very useful as a simple method to record changes in cell properties and reveal trends in their reactions to external stimuli, and also to correlate these signals with information obtained through other methods like optical microscopy, fluorescence imaging, and AFM.

In this study, cells were seeded in situ and they were monitored in real-time by simultaneous QCM-D and light microscopy as they attached and spread. The cells were subsequently treated with a cytoskeleton perturbing agent, and were finally allowed to recover (Fig. 1). The induced cytoskeleton changes were expected to be sensed by QCM-D as changes in viscoelastic properties of the layer of cells on the sensor surface. The drug-like, non-toxic compound cytochalasin D was chosen to induce changes in the cells, both due to its well-known cytomorphic effect on mammalian cells [40], and for being acting rapidly and reversibly upon wash out [41]. Importantly, the combined use of light microscopy facilitated correlation and interpretation of the QCM-D responses during the different phases of the experiment and allowed us to suggest a future strategy on how to represent the cell/surface interface and how this is affected by cytoskeletal rearrangements.

2 Materials and Methods

Materials were obtained from commercial sources, unless otherwise stated. Water was deionised (resistivity >18.2 mΩ cm,) and filtered using a MilliQ plus unit (Millipore, France). Phosphate-buffered saline (PBS) was prepared from tablets yielding a 0.01 M phosphate buffer, 0.0027 M potassium chloride and 0.137 M sodium chloride solution at pH 7.4 (Sigma) and used filtered and degassed (for QCM-D) or autoclaved (for cells).

2.1 Cell Culture

NIH3T3 fibroblasts (ECACC) were routinely cultured in Dulbecco's modified Eagle's Medium (DMEM) (Sigma) supplemented with 10 % calf serum (CS) (PAA laboratories), 1 mM sodium pyruvate (Sigma), 2 mM L-glutamine (Invitrogen), and 1 % penicillin streptomycin (Invitrogen). Human dermal fibroblasts (HS 483.T, ATCC) were

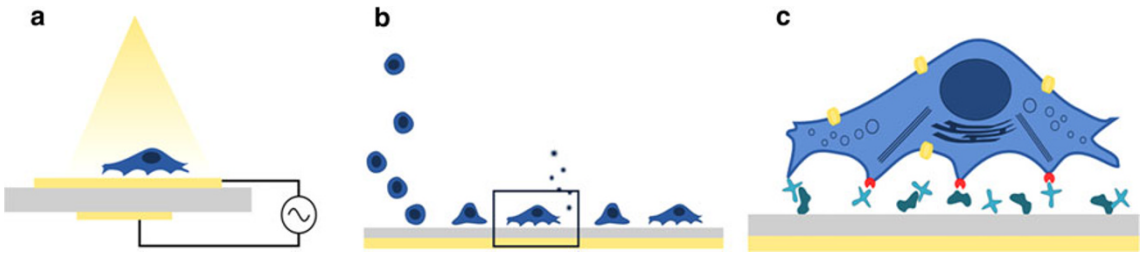

Fig. 1 Schematic illustration of the experimental design, using **a** a combined setup with a windowed QCM-D module mounted on a microscope. **b** The cells were seeded on the QCM-D sensor in situ where they were allowed to attach and spread. Their reversible responses due to rearrangements in the cytoskeleton (detailed in **c**) were followed in real-time

cultured in DMEM supplemented with 10 % fetal calf serum (FCS) (PAA laboratories), 1 mM sodium pyruvate, 2 mM L-glutamine, and 1 % penicillin streptomycin up to passage 6. For QCM-D experiments, cells were washed with warm PBS and dissociated with trypsin-EDTA solution (Invitrogen). The trypsin-cell suspension was centrifuged, with a washing step (2 ml of PBS), and re-suspended in filtered CO_2-independent medium (Invitrogen) supplemented as above containing a buffer system to keep the pH at 7.2–7.5 at ambient conditions.

2.2 QCM-D Experiments

The QCM-D experiments were performed using a Q-Sense E1 instrument equipped with a window module and SiO_2-coated QCM-D crystals with a fundamental frequency, f_0, of 5 MHz (Q-Sense, Västra Frölunda, Sweden). Measurements were recorded at several odd multiples of the fundamental frequency (overtones) and frequency shifts were normalised by division with the overtone number. Between measurements, crystals were stored in a 10 mM sodium dodecyl sulphate (SDS) solution. Prior to mounting, the crystals were sonicated 10 min each in the SDS solution and in water, dried under streaming N_2, and exposed to UV-O_3 for 15 min. The experiments were performed at 37 °C, in flow mode, and all solutions were equilibrated in a 37 °C water bath before being introduced into the measurement chamber to avoid formation of gas bubbles in the measurement chamber. Surface preparation steps were performed at 100 µl/min and cell steps at 50 µl/min. The crystal was equilibrated in PBS prior to adsorption of collagen I or fibronectin (Sigma; 10 µg/ml in PBS). The adsorbed protein was rinsed with PBS, and then exposed to the serum-containing medium. When a stable baseline had been obtained in medium, cells were flowed to the sensor (2–5 $\times$ 10^5 cells/ml) and their distribution was monitored by polarised light microscopy with a Leica DM4000M equipped with a 10×, NA 0.25 BD N Plan Epi objective. The imaged area was selected close to the middle of the sensor surface, where the sensitivity is the highest. When cells were visibly flowing over the surface, the flow was stopped briefly ($\sim$2 min) allowing cells to sediment, at which point the flow was resumed with cells, until adequate surface coverage was achieved, and then switched back to medium without cells. Cells were allowed to attach under flow conditions. After 60–80 min the cells were exposed to cytochalasin D (Sigma, 2 µg/ml) (in medium) for 20 min. The cytochalasin D was washed out and the cells were allowed to recover for an hour prior to a second 20 min exposure. Cell morphology was monitored and imaged by polarised light microscopy throughout the QCM-D measurement. The effect of the cytochalasin D treatment was characterised as the maximal dissipation shift due to the cytochalasin D exposure divided by the dissipation shift due to cells.

When QCM measurements are performed in gas phase, the resonance frequency shift, Δf, of the quartz resonator due to the presence of a thin layer on the sensor surface is proportional, with high accuracy, to the layer mass M, according to the Sauerbrey relation [42]:

$$\Delta f = -f_0 M / m_q \tag{1}$$

where m_q is a surface mass of the naked quartz crystal. This estimation is independent of the elastic properties of the layer. For elastic layers of finite thickness, the Sauerbrey relation must be corrected to include the shear elastic modulus G of the layer material. For soft, viscoelastic layers not only shear elasticity (storage modulus G_S) but also viscosity (loss modulus G_L) components of the complex shear modulus G^* must be taken into account:

$$G^* = G_s + iG_L \tag{2}$$

Based on continuum mechanics, equations have been derived which relate frequency and dissipation shifts sensed by QCM-D to changes in G_S and G_L for viscoelastic layers represented by Voight elements [12]. These equations are commonly used for QCM-D data evaluation.

3 Results

In this study, our primary aim was to investigate how deliberately induced cytoskeletal changes in cells, attached

to a QCM-D sensor, affect the measured QCM-D responses, i.e., the resonance frequency and dissipation shifts, Δf and ΔD, respectively. The QCM-D responses are expected to be affected, since cytoskeletal changes in turn induce changes in cell attachment and/or in the viscoelastic properties of attached cells, which in turn affect the coupled mass (Δf) and the viscoelastic properties (ΔD). As a first step, a suitable protocol for the functionalisation of the sensors with cell attachment proteins was established, and the properties of this protein layer were studied. This was followed by protocols for cell seeding, attachment, and treatment. To increase the generality of the study, two types of fibroblasts were studied, the first being the commonly used NIH3T3 line, and the second being the HS483.T line, as a more organotypical cell type. These two cell types both meet the requirements to readily attach to suitably prepared surfaces, and to develop an organised cytoskeleton upon spreading within a suitable experimental time frame.

The measurements were performed as described in the following, and a typical QCM-D result is shown in Fig. 2. The substrate (i.e., the QCM-D sensor) was coated with extra-cellular matrix protein, and then equilibrated in CO_2-independent medium containing the relevant serum, as described in the first section below (first 30 min). Next, the cells were seeded in situ (at t = 30 min in Fig. 2), and their attachment and spreading (B and C, respectively, in Fig. 2) were followed in real-time by both QCM-D and microscopy, by using a window-equipped QCM-D module mounted in a light microscope. Finally, as described in the third section below, when the cells had been allowed to attach and spread for an hour, reversible morphological and viscoelastic changes were induced in the cells (at t = 110 min in Fig. 2) by addition of the cytomorphic agent cytochalasin D. The induced changes were followed with both techniques.

3.1 Preparation of QCM-D Sensors for Cell Attachment Studies

Fibroblasts are known to attach and spread on cell culture plates and glass slides modified with ECM proteins following conventional protocols. Therefore, as a first measure in our study, the adsorption of collagen I and fibronectin to SiO_2 coated QCM-D sensors and the subsequent interaction with cell medium was measured by QCM-D, as exemplified in the two adsorption steps (during the first 30 min of the experiment) in Fig. 2, prior to the addition of cells (indicated by A).

Adsorption of either collagen I or fibronectin to the sensor surface yielded significant negative frequency shifts and positive dissipation shifts (Table 1), which increased further in magnitude upon the subsequent adsorption of

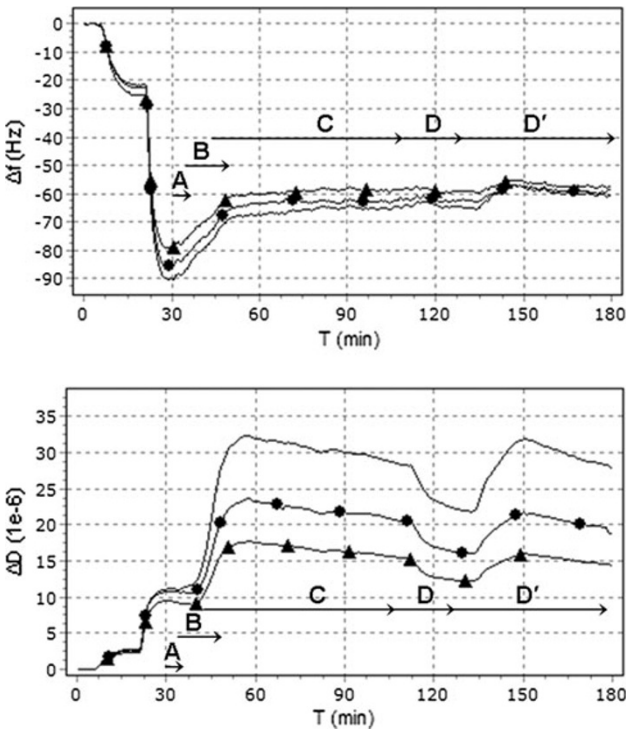

Fig. 2 QCM-D frequency and dissipation versus time curves for 3T3 cells added to surfaces modified by collagen I ($0 < t < 13$ min) and exposed to CO_2 independent medium containing 10 % CS ($18 < t < 30$ min). The protein coated surfaces were subjected to (*A*) cell seeding, (*B*) cell attachment, and (*C*) cell spreading (these regimes were assigned by real-time microsopy), after which the effect of (*D*) the addition of cytochalasin D (2 μg/ml) followed by (*D′*) rinsing with medium leading to cell recovery was monitored. The 3rd (*line*), 5th (*circle*), and 7th (*triangle*) overtones are shown

proteins from serum-containing medium. These results indicate, as expected, the formation of a soft (based on the $\Delta D/\Delta f$ ratio) and highly hydrated protein layer on the sensor surface prior to the addition of cells. The mass of the absorbed protein layer, as measured by QCM-D, includes both the biomolecular mass and the amount of water (buffer), which is acoustically coupled to the oscillations of the QCM-D sensors, and it was found that the adsorbed mass more than doubled as serum proteins adsorbed to the collagen I or fibronectin coated surface. Based on previous studies, we estimate the water content of these films (corresponding to a mass on the order of 1 μg/cm^2 as estimated by the Sauerbrey equation) to be high (>50 %). The positive frequency shift between 30 and 45 min (loss of dynamically coupled mass) may indicate spontaneous structural rearrangements of the underlying proteins including release of water (see below).

In separate experiments, the bulk effect of the medium without serum proteins added to it was evaluated, and showed that the bulk contribution to the cell medium step was small ($\Delta f_3 = -4 \pm 0.25$ Hz, $\Delta D_3 = (1.9 \pm 0.5) \times 10^{-6}$, n = 2). Furthermore, no bulk shifts (changes in the

Table 1 Average QCM-D frequency (Δf) and dissipation (ΔD) shifts obtained for adsorption from the protein solution and medium preparations used

Component	Δf_3 (Hz)	ΔD_3 (10^{-6})	n
Collagen I (10 μg/ml, PBS)	−36.4 ± 7.4	6.3 ± 2.5	6
Fibronectin (10 μg/ml, PBS)	−28.0 ± 2.8	1.7 ± 0.4	2
Medium + 10 % FCS on collagen I	−43.9 ± 6.2	5.0 ± 2.7	4
Medium + 10 % FCS on fibronectin	−40.8 ± 4.6	5.9 ± 0.8	2
Medium + 10 % CS on collagen I	−32.5 ± 0.7	3.3 ± 3.9	2

Mean with SD were calculated from n experiments

frequency and dissipation due to the change in solution, i.e., from buffer to media) or other effects on a cell-free protein layer were detected upon addition of media containing cytochalasin D (the QCM-D data are shown in Fig. S1 in the supplementary information).

3.2 Monitoring of Cell Attachment in the Window Equipped QCM-D Flow Cell

Several practical issues arising from working with live cells in the QCM-D window module were identified and solved, related to preheating of samples and the cell seeding procedure (see Sect. 2). By microscopy, it was evident that cells were attaching to the protein modified sensor surfaces. Whilst only minor changes were observed in the frequency signal, when cells attached, strong responses were observed in the dissipation signal, as can be seen in the example with 3T3 cells in Fig. 2 after cell seeding (indicated by A), where there is an immediate and strong increase in dissipation indicating the onset of cell attachment (indicated by B) and subsequently spreading (indicated by C). These different phases were determined by real-time microscopy and partly overlapped. In the figure, results for three different overtones are shown, and it can be seen that the magnitude of the dissipation shift is dependent on the overtone used (higher magnitude dissipation shifts were obtained for lower overtone numbers), which is consistent with what has been reported before, for cells [31] as well as for bacteria [43].

The cells were allowed to spread for an hour, without external interference. During the spreading phase, the frequency remains constant but the dissipation is slightly reduced ($\Delta f = 0$ Hz, $\Delta D = -3.5 \times 10^{-6}$). Despite efforts to ensure even cell spreading over the surface, there was an uneven spatial distribution over the sensor. Similar to 3T3 cells, HS483.T cells showed a strong signal in the dissipation, however without the slight drop during the spreading phase (see supplementary information, Fig. S3).

The different phases of the cell seeding, attachment, and spreading to the protein modified surfaces are also indicated in the so called *Df*-plots in Fig. 3 (corresponding to Fig. 2), where the dissipation shift is plotted as a function of the frequency shift. The $\Delta D/\Delta f$ ratio emphasises the structural properties of the layer and it can be seen in the leftmost part of the curves that the protein layer is compacted during the seeding phase (Δf increases without large effects in ΔD), whereas the later part of the attachment phase and the first part of the spreading phase are characterised by a distinct regime in the *Df*-plot where an increasingly soft film is formed until the cells reach an equilibrium state where the *Df* curves level out. Thus, from the QCM-D data, it is tempting to define a regime corresponding to the formation of adhesion points between the cell and the surface, which does not distinguish attachment from spreading. Such an interpretation makes sense given the short penetration depth of QCM-D compared to the cell dimensions.

3.3 Viscoelastic and Morphological Changes in Cells Upon Cytoskeletal Rearrangements

As can be seen in Fig. 4 (left), after being at the surface for an hour, the majority of the cells had attached and spread on the collagen I and serum coated QCM-D sensor. Some of the cells that had not initiated spreading immediately (arrows), remained round for the entire duration of the measurement, whereas others appeared to be triggered to spread by either the first or second cytochalasin D treatment.

Exposure to cytochalasin D induced drastic changes in the cell morphology (retraction/rounding of the cell body) as seen in Fig. 4 (middle picture), and a significant decrease in dissipation when cells were present (Fig. 2), but did not have any effect on a cell-free layer (see the supplementary information, Fig. S1). The effect on the cells (and the corresponding dissipation shifts) was reversible on wash out with medium. We noted that although the bulk of the cell body retracts when exposed to cytochalasin D (middle picture in Fig. 4), the area of the cell in contact with the substrate appears to remain the same. The insert (middle picture) is an enlarged image of a cell in the lower left corner of the image series, showing the retraction, or collapse of the cell body after exposure to cytochalasin D. Similar results were obtained for both cell types.

We quantified the effect of the cytochalasin D treatment through the value of the maximal dissipation shift caused by the cytochalasin exposure divided by the dissipation shift due to cells (taken just prior to the addition of cytochalasin D). According to this quantity, the effect of cytochalasin D treatment is larger for lower overtones, pointing towards that most of the change in the cells is sensed further away from the sensor surface. Specifically, 46 ± 4 and 45 ± 13 % reductions of the dissipation signal

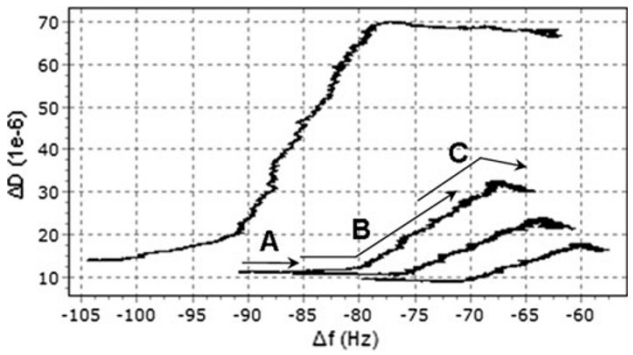

Fig. 3 QCM-D *Df* plot for 3T3 cells on collagen. *Arrows* indicate (*A*) seeding, (*B*) attachment, and (*C*) spreading phases as distinct regimes within each plot. The 1st, 3rd, 5th and 7th overtone data series are presented from *left* to *right* (*decreasing* absolute D shifts)

were observed at the third overtone for the 3T3 ($n = 3$) and the HS483.T fibroblasts ($n = 2$), respectively. It is interesting to note that the reorganization of the cell in response to cytochalasin D is represented by a similar *Df*-plot as the regime in Fig. 3 suggested to correspond to the formation of adhesion points (see above). Thus it seems not to be the formation of the focal adhesion points as such which give rise to the QCM-D response but rather the changes of the properties of the cell itself (bulk or lower part of the cell) when going from the spread state to the retracted (or attached) state or vice versa.

The benefit of combining QCM-D and microscopy is illustrated by how the QCM-D results were more distinct with the 3T3 cells whereas the light microscopy results were more apparent for the HS483.T cells. The reason for this is the more homogenous attachment of the 3T3 cells over the whole QCM-D sensor surface area, whereas the HS483.T cells were more easily imaged due to their larger size.

4 Discussion

The interface between a cell and its substrate, i.e., the extracellular part, may have a thickness of less, or much less, than 100 nm. Thus, two cells that look very similar in microscopy may still have very different such interfacial properties. This highlights the need to combine microscopy with other methods. This is one reason that the QCM-D technique has become increasingly popular for studying cell surface interactions and cells at surfaces. For example, it has been shown that whilst fluorescence images of cells on QCM-D sensors looked very similar for different situations/conditions, the corresponding QCM-D *Df* profiles were different and possibly indicated differences in the attachment and spreading process between different surfaces [44]. However, there has been no consensus in the literature on the magnitude and sign of the QCM-D signals to be expected for cells (either mammalian or bacterial). This indicates that QCM-D data should not necessarily be interpreted as a direct measure of the number or mass of adherent cells, but rather as a measure of a convoluted set of properties of this adherent layer. This is also consistent with theoretical analyses of conventional viscoelastic layer models which suggest that there is no simple relationship between e.g., the number of cells (or cell layer thickness) and the expected Δf and ΔD responses. For example, in previous studies where the sequential build-up of liposome multilayers on a QCM-D sensor surface was monitored, a change in sign of the frequency response in thick films (>100 nm) was observed while the dissipation still increased in magnitude [45].

The system in this study, cells attached to a surface, represent a thick layer (approximated to 10 μm) from a QCM-D point of view. We stipulate that the cells in the

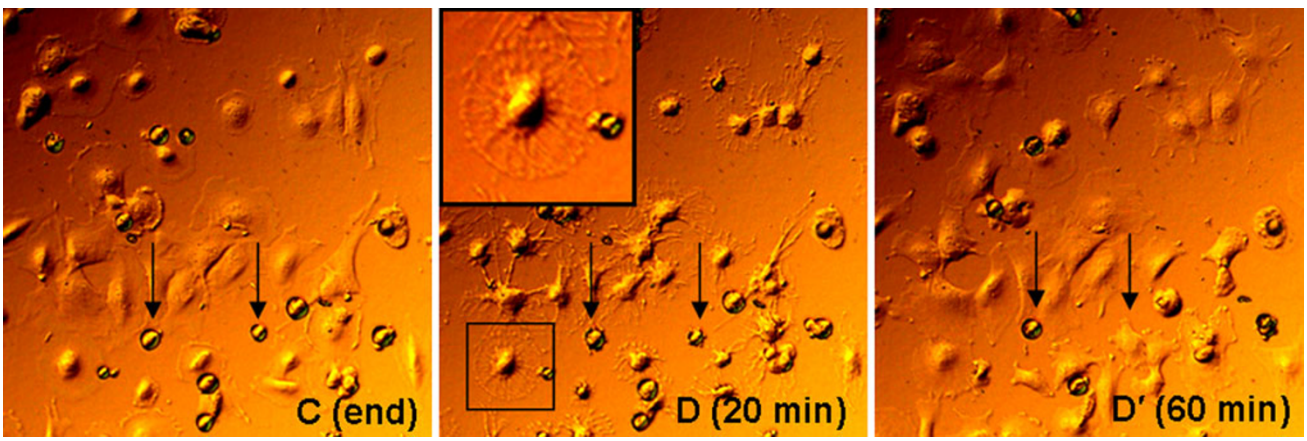

Fig. 4 Live cell images of HS 483.T on collagen and serum coated QCM sensors show (*left*) cell spreading prior to cytochalasin D treatment, (*middle*) cell retraction after 20 min exposure to cytochalasin D, including a ×2 magnified insert of a single cell, and (*right*) recovery of spread morphology over an hour. Images were taken close to the *middle* position of the QCM crystal, where the sensitivity in the QCM-D measurement is the highest

simplest form should be represented as an acoustically 'thick' layer, typically a few microns, which is much larger than the characteristic penetration depth δ ($\delta \approx 0.25$ μm in water at $f_0 = 5$ MHz) of the shear acoustic waves (Fig. 5). Thus, a dense layer of cells on the sensor surface can be viewed as a 'bulk' material, where the mechanical properties of water above the cell layer do not influence the frequency and the dissipation changes. In contrast, the properties of the cell bulk material will generally have a large influence on the QCM-D responses. The cell is a complex composite material where the cytoskeleton provides mechanical support to the cell and it is also involved in signal transduction. The shear elasticity of the cytoskeleton plays a key role in cell mechanical properties [46], and thus the changes in cytoskeleton viscoelasticity can lead to changes in both Δf and ΔD characteristics. In fact, the alteration in stiffness or softness of the cytoskeleton can influence the QCM-D characteristics to the same extent or even more than the changes in the surface mass (also dependent on cell density).

In the present study, we do not make an attempt to quantitatively model the results that we obtained. This is not possible with currently available models, which would need to take into account more profound heterogeneities both laterally along the surface and perpendicular to the surface. Nevertheless, we propose that cells on QCM-D sensor surfaces for discussion and analysis purposes, and especially to discuss trends, can meaningfully be represented by a two-layer-model (Fig. 5), as an extension of the one-layer-model, which is commonly used to model QCM-D data [11, 12, 47, 48]. In this model, the interior of the cells is represented by a soft, homogenous layer. This

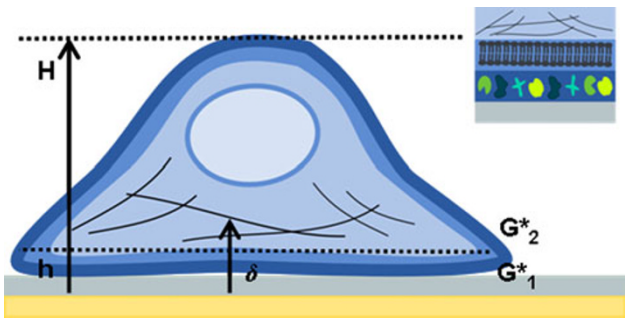

Fig. 5 Schematic illustration (not to scale) of the two-layer-viscoelastic model suggested as a simplified representation of QCM-D responses in cell experiments. The interfacial layer between the cell and the sensor surface (index '1') represents the structures responsible for the cell adhesion to the sensor surface, including the sensor coating, any material present between the sensor coating and the cell, the cell membrane, and material inside the cell associated with the cell membrane (shown in *upper insert*). The top layer (index '2') approximates the bulk properties of the cell. H denotes maximal cell thickness estimated at ~10 μm, h the thickness of the interfacial layer and δ the penetration depth (sub-micrometer)

approximation is less suitable when modelling, e.g., bacterial adhesion, where the bacteria show rigid, particle-like geometry and where a model based on coupled oscillators may be better [49]. The interfacial layer (index '1') is an "effective medium" that represents the surface-contacting part of the cells, as well as material present between the cell and the sensor surface (i.e., the sensor surface coating and extra-cellular matrix proteins), underneath a viscoelastic layer of a thickness close to that of the cell (index '2'). The interfacial layer is assumed to be of thickness $h \ll$ H and to be an acoustically thin film ($h \ll \delta$). The two layers are characterised by their complex shear elastic moduli, G_1* and G_2*. Since the cell is acoustically a bulk medium it can be considered as a semi-infinite medium.

In our experiments, the cell attachment step yielded positive frequency and dissipation shifts. The former is counter intuitive based on the Sauerbrey equation (Eq. 1) since mass is added to the sensor. One way to rationalise these results is by realising that the bulk mass of the cells is outside the penetration depth of the QCM-D shear wave and thus do not influence the oscillating frequency. However, from the large dissipation increase upon cell adhesion it is clear that the cells do interact with the interfacial layer.

Similarly, changes in the thickness of the cells resulting for the morphological changes during the second part of the experiment, where cytochalasin D was added, yielded only very weak frequency responses whereas at the same time inducing large changes in the dissipation shifts. We observed up to 50 % reduction in the dissipation signal (~20 % of the cumulative dissipation) upon exposure of the cells to cytochalasin D (at the 3rd overtone), and an enhanced maximal dissipation after wash out of cytochalasin D, where cells were also observed to spread more rapidly. A model of the cell as a viscous adhesive cortical shell enclosing a less viscous interior, which becomes more uniformly viscous after treatment with cytochalasin D has been described [50], and illustrates how this enhanced spreading may happen.

Taken together, we suggest changes in cell viscoelastic properties to be the main determinant for the QCM-D responses in our experiments. However, we cannot rule out that the (changes in the) elastic properties of the extracellular matrix layer between the cell and the substrate may also play a significant role (Fig. 5). This layer provides a direct mechanical coupling between the underlying matrix/sensor surface and the cell cytoskeleton once the cell has begun forming focal adhesions. This coupling allows the cells to probe their local environment by "pulling/pushing" on the adhesion sites. When the cells are treated with cytochalasin D, and the integrity of the actin mesh is altered, the mechanical interaction between the cell and the protein layer must change, as well as the viscoelastic properties of the cell itself. It is also possible that the

QCM-D signals could pick up the mechanical coupling between the sensor surface and the cytoskeleton. It is therefore interesting to extend the theoretical modelling, to identify conditions where the contribution from the layer between the cells and the support will be important, after which experiments can be designed to test these predictions.

Whilst much of the prior work related to the present study so far has been done looking at cell attachment and spreading, QCM-D has also been used to look at other aspects of cells such as stimulated exocytosis [51], toxicity [35], and receptor signaling-mediated changes in the cytoskeleton [36]. Since it is known that the mechanical properties of cells are tightly linked with cell fate processes, it is possible that QCM-D has potential for use, alone or in combination with other techniques such as impedance and electrochemistry type measurements, in monitoring, e.g., differentiation via contractile properties of the cells, and also as a potential cell-based drug screening method. It is our opinion that future cell studies by QCM-D would greatly benefit from systematic studies aiming to understanding of how to predict QCM-D responses originating from cells undergoing morphological transformations.

5 Conclusions

We measured reproducible QCM-D signals originating from fibroblast attachment to collagen and fibronectin modified surfaces, whilst doing light microscopy. Cell attachment and spreading resulted in minor positive frequency shifts, and was associated with large dissipation shifts. The attached fibroblasts responded reversibly to the cytomorphic agent cytochalasin D by retraction of the cell body, clearly seen in the microscopy images, and also detected as large dissipation shifts in QCM-D. We conclude that viscoelastic changes in the cells would result in closely interlinked changes in cell bulk properties and properties of the interfacial layer between the cell and the substrate, and that which of these contribution that dominates the QCM-D signals cannot be determined without further development of a mechanical model for cells at the sensor surface.

Acknowledgments The authors gratefully acknowledge input from Dr. Christina Gretzer, AstraTech, Mölndal, Sweden, as well as funding from the EU 7th Framework Programme (FP7/2007-2013) under grant agreement no NMP4-SL-2009-229292 (Find and Bind).

References

1. Vogel V, Sheetz M (2006) Nat Rev Mol Cell Biol 7(4):265–275
2. Pelham RJ, Wang YL (1997) Proc Nat Acad Sci USA 94(25):13661–13665
3. Chen CS, Mrksich M, Huang S, Whitesides GM, Ingber DE (1997) Science 276(5317):1425–1428
4. Choquet D, Felsenfeld DP, Sheetz MP (1997) Cell 88(1):39–48
5. Riveline D, Zamir E, Balaban NQ, Schwarz US, Ishizaki T, Narumiya S, Kam Z, Geiger B, Bershadsky AD (2001) J Cell Biol 153(6):1175–1185
6. Tymchenko N, Wallentin J, Petronis S, Bjursten LM, Kasemo B, Gold J (2007) Biophys J 93(1):335–345
7. Rodahl M, Kasemo B (1996) Rev Sci Instrum 67(9):3238–3241
8. Martin SJ, Granstaff VE, Frye GC (1991) Anal Chem 63:2272–2281
9. Johannsmann D, Mathauer K, Wegner G, Knoll W (1992) Phys Rev B: Condens Matter 46:7808–7815
10. Johannsmann D (2007) Studies of viscoelasticity with the QCM. In: Steinem C, Janshoff A (eds) Piezoelectric Sensors, vol 5. Springer- Verlag, New York, pp 151–170
11. Domack A, Prucker O, Ruhe J, Johannsmann D (1997) Phys Rev E Stat Phys Plasmas Fluids Relat Interdiscip Topics 56(1): 680–689
12. Voinova MV, Rodahl M, Jonson M, Kasemo B (1999) Phys Scr 59(5):391–396
13. Lucklum R, Hauptmann P (2006) Anal Bioanal Chem 384:667–682
14. Kanazawa K, Frank CW, Hardesty J (2008) ECS Trans 16:419–429
15. Hovgaard MB, Rechendorff K, Chevallier J, Foss M, Besenbacher F (2008) J Phys Chem B 112(28):8241–8249
16. Jensen T, Dolatshahi-Pirouz A, Foss M, Baas J, Lovmand J, Duch M, Pedersen FS, Kassem M, Bunger C, Soballe K, Besenbacher F (2010) Colloids Surf B 75(1):186–193
17. Kohen NT, Little LE, Healy KE (2009) Biointerphases 4(4): 69–79
18. Holst J, Watson S, Lord MS, Eamegdool SS, Bax DV, Nivison-Smith LB, Kondyurin A, Ma LA, Oberhauser AF, Weiss AS, Rasko JEJ (2010) Nat Biotechnol 28(10):1123–1168
19. Svedhem S, Dahlborg D, Ekeroth J, Kelly J, Hook F, Gold J (2003) Langmuir 19(17):6730–6736
20. Thid D, Bally M, Holm K, Chessari S, Tosatti S, Textor M, Gold J (2007) Langmuir 23(23):11693–11704
21. Huang X, Zauscher S, Klitzman B, Truskey GA, Reichert WM, Kenan DJ, Grinstaff MW (2010) Ann Biomed Eng 38(6): 1965–1976
22. Andersson AS, Glasmastar K, Sutherland D, Lidberg U, Kasemo B (2003) J Biomed Mater Res 64A(4):622–629
23. Huang CJ, Tseng PY, Chang YC (2010) Biomaterials 31(27):7183–7195
24. Mhanna RF, Voros J, Zenobi-Wong M (2011) Biomacromolecules 12(3):609–616
25. Saitakis M, Gizeli E (2012) Cell Mol Life Sci 69(3):357–371. doi:10.1007/s00018-011-0854-8
26. Redepenning J, Schlesinger TK, Mechalke EJ, Puleo DA, Bizios R (1993) Anal Chem 65(23):3378–3381
27. Gryte DM, Ward MD, Hu WS (1993) Biotechnol Prog 9(1): 105–108
28. Fredriksson C, Khilman S, Kasemo B, Steel DM (1998) J Mater Sci Mater Med 9(12):785–788
29. Nimeri G, Fredriksson C, Elwing H, Liu L, Rodahl M, Kasemo B (1998) Colloids Surf B 11(5):255–264
30. Fredriksson C, Kihlman S, Rodahl M, Kasemo B (1998) Langmuir 14(2):248–251

31. Modin C, Stranne AL, Foss M, Duch M, Justesen J, Chevallier J, Andersen LK, Hemmersam AG, Pedersen FS, Besenbacher F (2006) Biomaterials 27(8):1346–1354
32. Saravia V, Toca-Herrera JL (2009) Microsc Res Tech 72(12):957–964. doi:10.1002/jemt.20742
33. Satriano C, Messina GM, Marino C, Aiello I, Conte E, La Mendola D, Distefano DA, D'Alessandro F, Pappalardo G, Impellizzeri G (2010) J Colloid Interface Sci 341(2):232–239
34. Lord MS, Modin C, Foss M, Duch M, Simmons A, Pedersen FS, Besenbacher F, Milthorpe BK (2008) Biomaterials 29(17):2581–2587. doi:10.1016/j.biomaterials.2008.03.002
35. Fatisson J, Azari F, Tufenkji N (2011) Biosens Bioelectron 26(7):3207–3212
36. Chen JY, Li MH, Penn LS, Xi J (2011) Anal Chem 83(8):3141–3146
37. Yang RG, Chen JY, Xi N, Lai KWC, Qu CG, Fung CKM, Penn LS, Xi J (2012) Exp Cell Res 318(5):521–526. doi:10.1016/j.yexcr.2011.12.003
38. Voinova MV, Jonson M, Kasemo B (2002) Biosens Bioelectron 17(10):835–841
39. Voinova M (2009) J Sens 13
40. Schliwa M (1982) J Cell Biol 92(1):79–91
41. Higuchi C, Nakamura N, Yoshikawa H, Itoh K (2009) J Bone Miner Metab 27(2):158–167
42. Sauerbrey G (1959) Zeitschrift Fur Physik 155(2):206–222
43. Olsson ALJ, van der Mei HC, Busscher HJ, Sharma PK (2009) Langmuir 25(3):1627–1632. doi:10.1021/la803301q
44. Lord MS, Modin C, Foss M, Duch M, Simmons A, Pedersen FS, Milthorpe BK, Besenbacher F (2006) Biomaterials 27(26):4529–4537
45. Graneli A, Edvardsson M, Hook F (2004) Chem Phys Chem 5(5):729–733
46. Mofrad MRK (2009) Annu Rev Fluid Mech 41:433–453
47. Rodahl M, Höök F, Fredriksson C, Keller CA, Krozer A, Brzezinski A, Voinova MV, Kasemo B (1997) Faraday Discuss 107:229–246
48. Voinova MV, Jonsson M, Kasemo B (1997) J Phys Condens Matter 9:7799–7808
49. Olsson ALJ, van der Mei HC, Busscher HJ, Sharma PK (2011) J Colloid Interface Sci 357(1):135–138. doi:10.1016/j.jcis.2011.01.035
50. Cuvelier D, Thery M, Chu YS, Dufour S, Thiery JP, Bornens M, Nassoy P, Mahadevan L (2007) Curr Biol 17(8):694–699
51. Cans AS, Hook F, Shupliakov O, Ewing AG, Eriksson PS, Brodin L, Orwar O (2001) Anal Chem 73(24):5805–5811. doi:10.1021/ac010777q